# Cholinergic Direct Inhibition of *N*-Methyl-D Aspartate Receptor-Mediated Currents in the Rat Neocortex

**JORGE FLORES-HERNANDEZ,[1] HUMBERTO SALGADO,[2] VICTOR DE LA ROSA,[1] TANIA AVILA-RUIZ,[1] OSWALDO TORRES-RAMIREZ,[1] GUSTAVO LOPEZ-LOPEZ,[1] AND MARCO ATZORI[2]***

[1]*Instituto de Fisiologia, Universidad Autonoma de Puebla, Puebla, Mexico*

[2]*Laboratory of Synaptic and Cell Physiology, University of Texas at Dallas, School of Behavioral and Brain Sciences, Richardson, Texas 75080*

*KEY WORDS* acetylcholine; NMDA; patch-clamp; auditory cortex; muscarinic; nicotine

*ABSTRACT* Acetylcholine (ACh) and *N*-methyl-D aspartate receptors (NMDARs) interact in the regulation of multiple important brain functions. NMDAR activation is indirectly modulated by ACh through the activation of muscarinic or nicotinic receptors. Scant information is available on whether ACh directly interacts with the NMDAR. By using a cortical brain slice preparation we found that the application of ACh and of other drugs acting on muscarinic or nicotinic receptors induces an acute and reversible reduction of NMDAR-mediated currents ($I_{NMDA}$), ranging from 20 to 90% of the control amplitude. The reduction displayed similar features in synaptic $I_{NMDA}$ in brain slices, as well as in currents evoked by NMDA application in brain slices or from acutely dissociated cortical cells, demonstrating its postsynaptic nature. The cholinergic inhibition of $I_{NMDA}$ displayed an onset–offset rate in the order of a second, and was resistant to the presence of the muscarinic antagonist atropine (10 μM) in the extracellular solution, and of G-protein blocker $GDP_{\beta}S$ (500 μM) and activator $GTP_{\gamma}S$ (400 μM) in the intracellular solution, indicating that it was not G-protein dependent. Recording at depolarized or hyperpolarized holding voltages reduced NMDAR-mediated currents to similar extents, suggesting that the inhibition was voltage-independent, whereas the reduction was markedly more pronounced in the presence of glycine (20 μM). A detailed analysis of the effects of tubocurarine suggested that at least this drug interfered with glycine-dependent NMDAR-activity. We conclude that NMDAR-mediated current scan be inhibited directly by cholinergic drugs, possibly by direct interaction within one or more subunits of the NMDAR. Our results could supply a new interpretation to previous studies on the role of ACh at the glutamatergic synapse. **Synapse 63:308–318, 2009.** 

## INTRODUCTION

*N*-methyl-D aspartate receptors (NMDARs) mediate excitatory transmission and are involved in synaptic function associated with long-term synaptic changes, oscillations, bursting behavior, learning, and memory (Burgos-Robles et al., 2007; Castellano et al., 2001; Chub et al., 1998; Nicoll and Malenka, 1999). Acetylcholine (ACh) released from terminals of neurons whose cell body are located in the Nucleus Basalis (Voytko, 1996; Voytko et al., 1994) modulates the behavior of many cortical areas by activation of muscarinic receptors (Mash and Potter, 1986) and nicotinic receptors (Alkondon and Albuquerque, 2004). Excitatory synaptic transmission in the primary auditory neocortex is subject to a particularly intense cholinergic modulation (Cox et al., 1992; Metherate and Ashe, 1991; Metherate and Ashe, 1993a,b, 1994; Metherate et al., 1990; Metherate and Weinberger, 1989, 1990). Cholinomimetics appear to have multiple

J. F.-H. and H. S. contributed equally to this work.

Contract grant sponsor: The NIH; Contract grant number: NIH5R01DC005986; Contract grant sponsor: NARSAD.

*Correspondence to: Marco Atzori, University of Texas at Dallas, School of Behavioral and Brain Sciences, 2601 North Floyd Road, Richardson, TX 75080, USA. E-mail: marco.atzori@utdallas.edu

Received 15 February 2008; Accepted 24 June 2008

DOI 10.1002/syn.20609

Published online in Wiley InterScience (www.interscience.wiley.com).

effects on NMDAR-mediated currents ($I_{NMDA}$): ACh increases $I_{NMDA}$ by acting on muscarinic and nicotinic receptors located in presynaptic terminals during the early postnatal period (P8-16) (Aramakis and Metherate, 1998; Aramakis et al., 1997, 1999), but decreases $I_{NMDA}$ in the retina (O'Dell and Christensen, 1988) and in primary neocortical neuronal cultures (Aizenman et al., 1991).

Less information is available on the cholinergic regulation of $I_{NMDA}$ after early development. In particular, it is not clear whether cholinomimetics interact directly with the NMDAR channel or rather the cholinergic inhibition is mediated by second messengers. By studying the cholinergic modulation of $I_{NMDA}$ in juvenile rats (P23-45), we found that ACh and other cholinergic, muscarinic and nicotinic agonists and antagonists, acutely and reversibly inhibited $I_{NMDA}$. The mechanism of the inhibition appeared to be postsynaptic, resulting directly from the interaction of the cholinergic drug or neurotransmitter with the NMDAR, and was not blocked by a G-protein blocker nor by the presence of the intracellular $Ca^{2+}$-chelator 1,2-bis(2-aminophenoxy)ethane-*N*,*N*,*N*′,*N*′-tetraacetic acid K (BAPTA-K), suggestive of a direct interaction between cholinergic drugs and the NMDAR.

## METHODS

### Preparation

We used an auditory cortex slice preparation similar to ones described earlier (Atzori et al., 2001, 2005). In some recordings, we used a medial prefrontal cortex slice preparation for a series of control experiments, as described previously (Atzori et al., 2001, 2005). Sprague Dawley rats of 23- to 45-day old (Charles River, Wilmington, MA) were anesthetized with forane (Baxter, Round Lake, IL), sacrificed according to the National Institutes of Health guidelines, and their brains sliced with a vibratome in a refrigerated solution (0–4°C) containing (mM): 130 NaCl, 3.5 KCl, 10 Glucose, 25 $NaHCO_3$, 1.25 $NaH_2PO_4$, 1.5 $CaCl_2$ and 1.5 $MgCl_2$, saturated with a mixture of 95% $O_2$ and 5% $CO_2$ (artificial cerebro-spinal fluid, ACSF). The recording solution contained also picrotoxin (100 μM) or bicuculline (10 μM) for blocking γ-aminobutyric acid A receptor ($GABA_AR$), dinitroquinoxaline (DNQX, 10 μM), and atropine (10 μM), for blocking α-amino-3-hydroxy-5-methyl-4-isoxazolepropionic acid receptor (AMPAR)-mediated currents, and muscarinic receptors, respectively, throughout the whole study. Coronal slices from the most caudal fourth of the brain were retained after removing the occipital convexity, and subsequently incubated in ACSF at 32°C before being placed in the recording chamber. The recording area was selected dorsally to the rhinal fissure corresponding to the auditory cortex (Rutkowski et al., 2003).

### Neuron dissociation

Brain slices were placed in an oxygenated cell-stir chamber containing papain (0.5 mg/mL, Sigma) at 35°C bubbled with $O_2$, titrated at pH = 7.4 with NaOH, 300–305 mOsm/L. After 20 min of enzyme digestion, tissue was rinsed three times with the low $Ca^{2+}$-isethionate solution and mechanically dissociated with a graded series of fire-polished Pasteur pipettes. The cell suspension was then plated into a 35-mm Lux Petri dish mounted on the stage of an upright fixed-stage microscope containing *N*-(2-hydroxyethyl)piperazine-*N*′-(2-ethanesulfonic acid) (HEPES)-buffered ACSF.

### Drugs and solutions

All drugs were purchased from Sigma (St. Louis, MO) or from TOCRIS (Ellisville, MO).

To assess a possible postsynaptic modulation, in some experiments, pulses of N-methyl-D aspartate (NMDA, 100 μm) were applied at 100–200 μm from the recording areas, once every 30 s. The NMDA was dissolved in distilled $H_2O$ and diluted tenfold in ACSF before being back-filled to a glass pipette similar to the one used for recording. NMDA application was performed with a pressure system (picospritzer, General Valve Corp. Fairfield, NJ) through a glass pipette (≅25 psi, 3–12 ms). Stock solutions of all drugs were prepared in water and drugs were either bath-applied or dispensed with a solenoid valve system with manifold application system with a dead time of <200 ms as measured in dissociated cells.

### Electrophysiology

#### Slice recording

Slices were placed in an immersion chamber, where cells with a prominent apical dendrite, suggestive of pyramidal morphology, were visually selected using an Olympus BX51 microscope (Olympus, Tokyo, Japan) with Nomarski optics and an infrared camera system (DAGE-MTI, Michigan City, IN). Excitatory postsynaptic currents (EPSCs) were recorded in the whole-cell configuration, in voltage clamp mode, with 3–5 MΩ electrodes filled with a solution containing (mM): 90 CsCl, 90 gluconic acid, 1 lidocaine *N*-ethyl bromide (QX314), 1 $MgCl_2$, 10 HEPES, 4 glutathione, 1.5 $ATPMg_2$, 0.3 $GTPNa_2$, 8 biocytin, 5 BAPTA-K, pH 7.2–7.3 with NaOH, and 275 mOsm/L. BAPTA blocks second messenger cascades caused by raises in intracellular calcium concentration (Beech, 1993; Jones et al., 1988; Vulfius et al., 1998). The holding voltage was not corrected for the junction potential (< 4 mV). Electrically evoked EPSC were measured by delivering two electric stimuli (90–180 μs, 10–50 μA) 100 ms-apart every 20 s with an isolation unit, through a glass stimulation monopolar electrode filled with

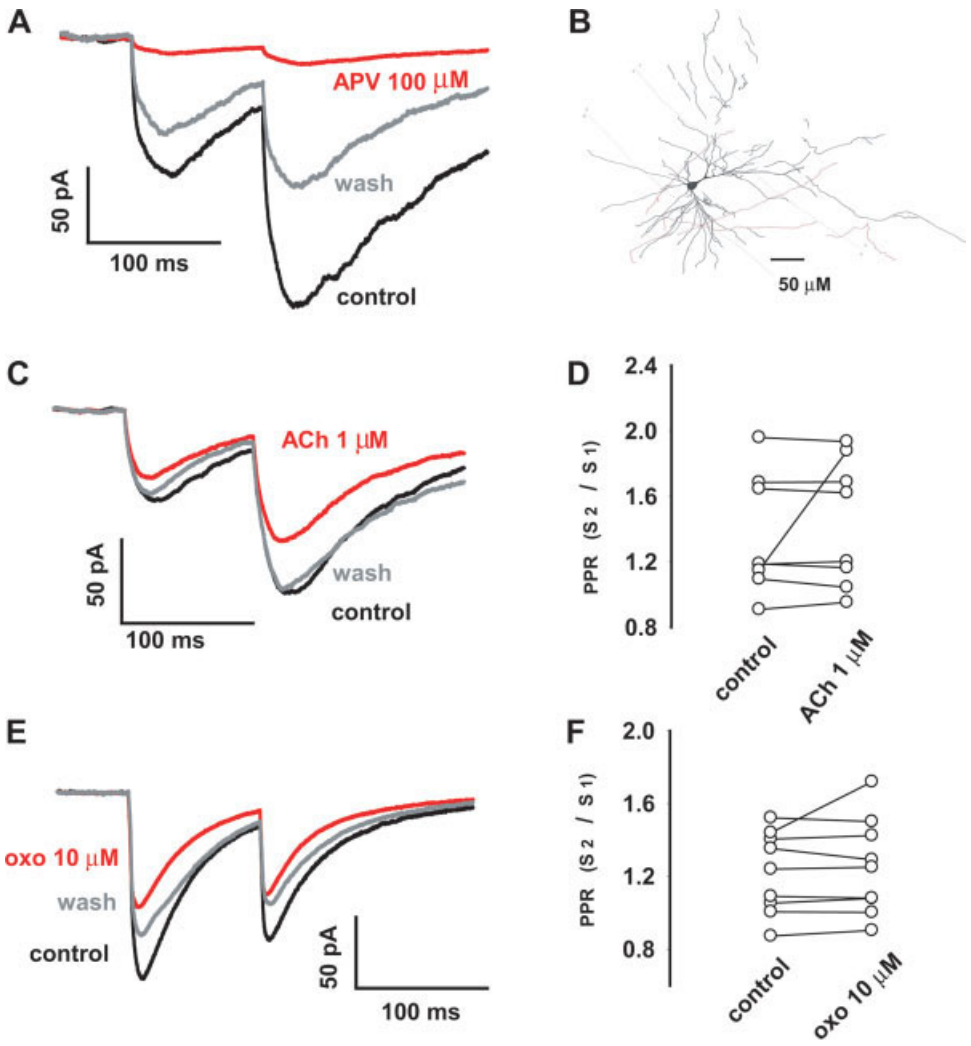


Fig. 1. Acetylcholine and oxotremorine inhibit electrically evoked NMDAR-mediated synaptic currents. **A**: NMDAR-mediated synaptic currents were evoked by stimulating afferents in layer II/III with an extracellular electrode and recording them in an ACSF solution containing AMPAR and $GABA_AR$ and muscarinic receptor blockers at $V_h = -40$ mV. A pair pulse protocol was used to measure the PPR. The current was blocked by 100 μM APV. **B**: Representative example of spiny neuron recorded in layer II/III. **C**, **D**: ACh (1 μM) inhibits postsynaptic $I_{NMDA}$ without changing PPR. Traces are the average of 10 individual responses recorded every 20 s. **E**, **F**: The muscarinic agonist oxotremorine (10 μM) produces an effect similar to ACh, also without change in PPR.

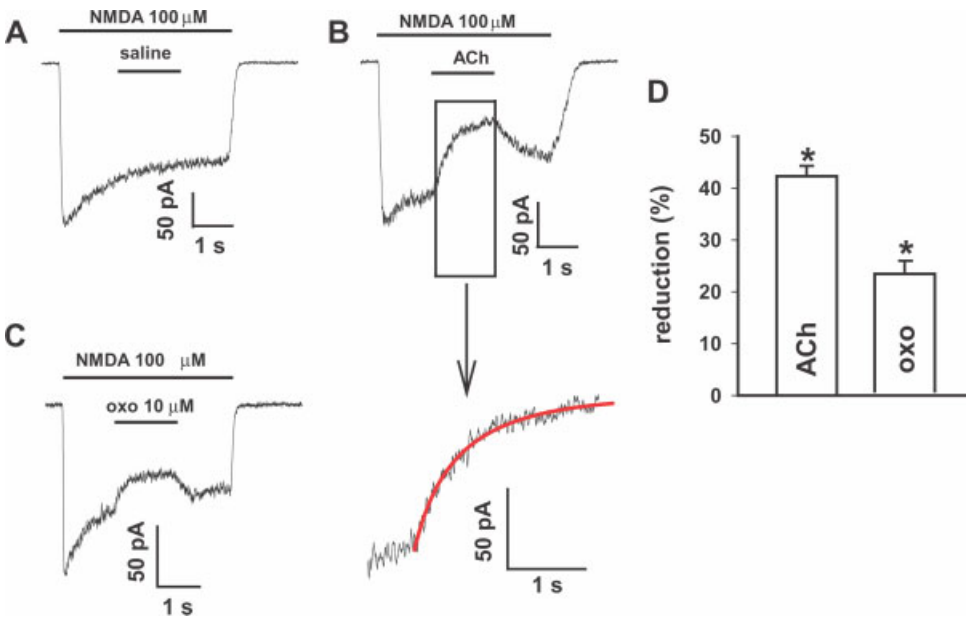


Fig. 2. Acetylcholine and oxotremorine inhibit chemically evoked NMDAR-mediated currents. **A**–**C**: Effect of application of ACSF, ACh or oxo on the current evoked by NMDA application in acutely dissociated neocortical neurons. Insert below (B) shows that the onset of the cholinergic block measured by an exponential curve with $\tau = 1089 \pm 28$ ms ($n = 11$). **D**: Bars indicate mean ± s.e.m. of the reduction by ACh or oxo ($n = 11$ and 8, respectively). The asterisk (*) indicates a statistically significant reduction ($P < 0.05$, Student's $t$-test).

artificial cerebrospinal fluid (ACSF) and placed in layer II/III, 150–200 μm from the recording electrode. EPSCs were blocked by aminophosphonovaleric acid (APV, 100 μM), confirming that they were mediated by NMDAR (Fig. 1A). Paired Pulse Ratio (PPR) was defined as the ratio between the mean of the second to the mean of the first response. $I_{NMDA}$ were induced by applications of NMDA itself (chemically evoked EPSCs (cEPSCs) in slices, in the presence of the $Na^+$-channel blocker tetrodotoxin (TTX, 1 μM), or from dissociated cell.

Recordings started after a stabilization period of a few minutes during which the pipette solution dialyzed into the recorded cell. We defined as statistically stable period a time interval along which the EPSC mean amplitude measured during any 5-min assessment did not vary according to an unpaired Student's *t*-test. After recording an initial baseline for more than 10 min, drugs were bath-applied for 5 min or longer, until reaching a stable condition (as defined earlier). In the case of recordings with a pipette solution containing the G-protein blocker $GDP_\beta S$ or activator $GTP_\gamma S$, we waited at least 20 min (on average ~30 min) before starting electrophysiological recording, in order to allow sufficient time to dialyze the cytosol with the intracellular solution. Drug effects were assessed by measuring and comparing changes between baseline (control) and treatment, with paired Student's *t*-tests (PPR, Wilcoxon's *t*-test). Analysis of variance (ANOVA) or unpaired Student's *t*-test were used for comparisons between different groups of cells. Data were reported as different only if $P < 0.05$. We indicated as $A_{contr}$ and $A_{treat(ment)}$ the mean amplitude of the glutamatergic currents in control or under the described treatment. The reduction was defined as $R \equiv 100 \times (1 - A_{treat}/A_{contr})$.

### Dissociated cell recordings

Whole-cell recordings employed standard techniques (Flores-Hernandez et al., 2002). Electrodes were pulled from Corning 8250 glass (A-M Systems, Inc, Carlsborg, WA) and heat polished prior to use. The internal solution consisted of (mM): 175 NMD glucamine, 40 HEPES, 2 $MgCl_2$, 10 Ethylene glycol-bis(γ-aminoethyl ether)-*N*,*N*,*N*′,*N*′-tetraacetic acid (EGTA), 12 phosphocreatine, 2 $Na_2ATP$, 0.2 $Na_2GTP$, 0.1 leupeptin, pH = 7.2–7.3 with $H_2SO_4$, 265–270 mOsm/L. The external solution consisted of (in mM): 127 NaCl, 20 CsCl, 5 $BaCl_2$, 2 $CaCl_2$, 12 glucose, 10 HEPES, 0.001 TTX, 0.02 glycine, pH = 7.3 with NaOH, 300–305 mOsm/L.

Recordings were obtained with an Axon Instruments 200A patch clamp amplifier and controlled with a Pentium clone running pClamp (v. 8.01) with a DigiData 1200 series interface (Axon Instruments, Foster City, CA). Electrode resistance was typically 2–4 MΩ in the bath. After seal rupture, series resistance (<20 MΩ) was compensated (70–90%) and periodically monitored. Recordings were made from pyramidal cells that had short (<75 μM) apical dendrites (Fig. 1B). Unless otherwise noted, the cell membrane potential was held at −80 mV.

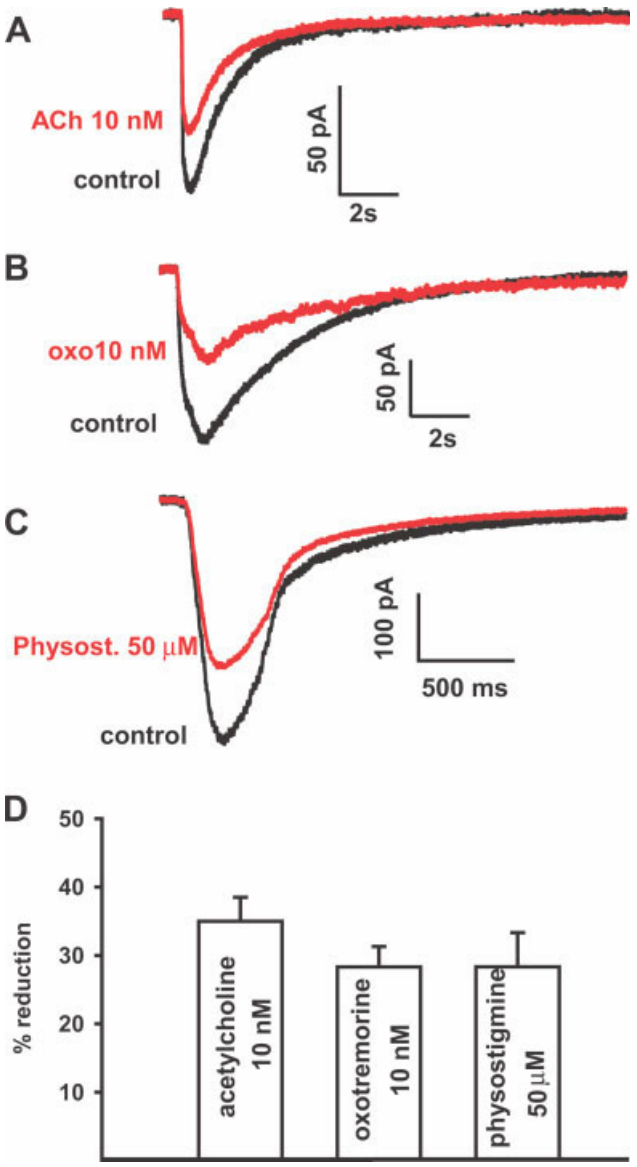


Fig. 3. The cholinergic inhibition of (cEPSC) $I_{NMDA}$ does not depend on G-proteins. Recordings performed in the presence of $GDP_\beta S$ in the intracellular solution. **A**,**B**: ACh (10 nM) or oxo (10 nM) decrease the current evoked by the pressure application of NMDA. **C**: The cholinesterase inhibitor physostigmine (50 μM) also reduces cEPSC. **D**: Effect of different treatments on $I_{NMDA}$, normalized to control. Compare mean ± s.e.m. of the effects of cholinomimetics in the presence of $GDP_\beta S$.

### Drug application

Drugs were applied with a gravity-fed "two-pipe" system. The array of application capillaries—glued at ~800 μm from each other—was positioned a few hundred μm from the cell under study. Solution were

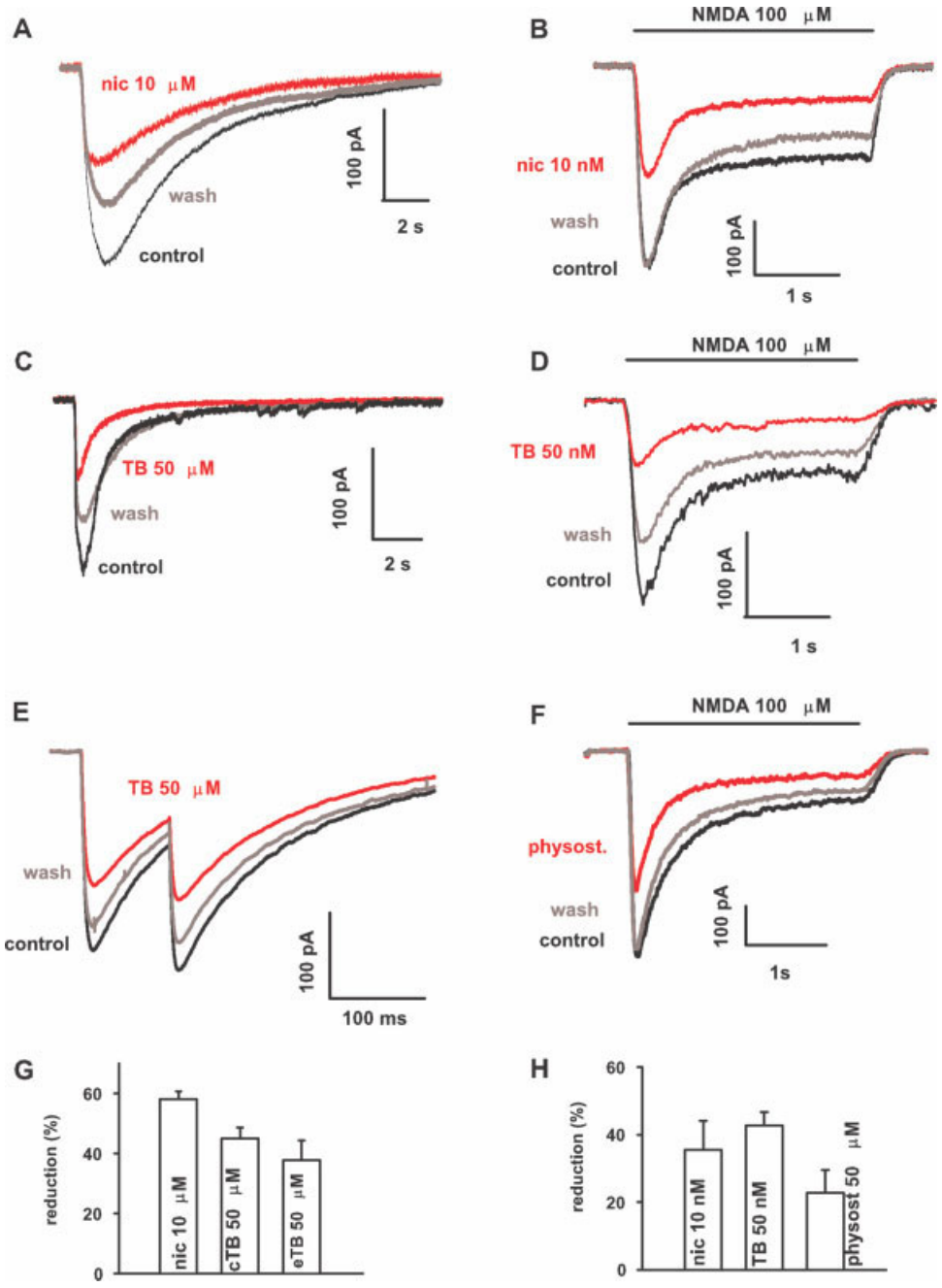


Fig. 4. Nicotine or tubocurarine inhibit $I_{NMDA}$. **A** and **B**: Representative traces showing that nicotine (10 μM) reduces chemically evoked $I_{NMDA}$ in brain slices (A) and nicotine (10 nM) in dissociated neurons (B), recorded at $V_h = -40$ mV. **C** and **D**: Representative trace showing that tubocurarine (TB, 50 μM) inhibits electrically evoked synaptic $I_{NMDA}$ (eEPSCs) in brain slices or dissociated cells (TB 50 nM), respectively. **E**: Tubocurarine also reversibly inhibits eEPSC. **F**: Representative trace illustrating the effect of physostigmine on chemically induced $I_{NMDA}$ in dissociated cells. **G**: Bar graphs report mean ± s.e.m. of the reduction in slices or dissociated cells, respectively. First and second column: reduction of chemically evoked $I_{NMDA}$ by 10 μM nicotine or 50 μM tubocurarine, respectively, third column, reduction of synaptic $I_{NMDA}$ by 50 μM tubocurarine. **H**: Inhibition of $I_{NMDA}$ by nicotine (10 nM) or tubocurarine (50 nM) and physostigmine (50 μM) in dissociated cells.

applied by changing the position of the array with a DC drive system controlled by a SF-77B perfusion system (Warner Instruments, Hamden, CT) synchronized by pClamp. The solution changes were complete within less than 100 ms. Generally, NMDA (1–1000 μM) was applied for 3 s every 20 s. Drugs were prepared as concentrated stocks in deoxygenated water.

## RESULTS

### Acetylcholine inhibits $I_{NMDA}$ postsynaptically

To study the effect of cholinergic drugs on synaptic $I_{NMDA}$ we recorded electrically evoked NMDA currents (eEPSCs) in the presence of DNQX (10 μM), bicuculline (10 μM) or picrotoxin (100 μM), and atropine (10 μM) in the control solution, at a holding potential of −40 mV, in order to remove $Mg^{2+}$ block. The NMDAR-mediated nature of the response was confirmed by complete block following the application of the NMDAR blocker aminophosphonovaleric acid (APV, 100 μM, Fig. 1A, $n = 3$). Neurons were injected with biocytin for posthoc identification. A cortical layer II biocytin-injected reconstructed neuron is shown in Figure 1B.

Application of ACh (1 μM) or of the muscarinic agonist oxotremorine (oxo, 10 μM) decreased eEPSCs amplitude ($R \equiv 100 \times (1 - A_{treat}/A_{contr}) = 36.4 \pm 6\%$

and 37.8 ± 6.3%, respectively, $n = 8$ each) without changing the pair pulse ratio (PPR) (PPR in control was 1.34 ± 0.13 vs. 1.43 ± 0.1 in ACh, $n = 8$, n.s, Wilcoxon's $t$-test; PPR = 1.22 ± 0.07 in control vs. 1.25 ± 0.09 in oxo, $n = 8$, n.s, Wilcoxon's $t$-test). In Figures 1C–1F, we show representative traces and PPR values illustrating the effect of ACh (C and D) and oxo (E and F). The invariance of the PPR following the application of ACh or oxo suggests, but does not prove, that the reduction of $I_{NMDA}$ is due to a postsynaptic effect.

To test whether the cholinergic-induced $I_{NMDA}$ inhibition was due to postsynaptic modulation we used a fast drug application system to apply the prototypical agonist NMDA (100 μM, chemically evoked or cEPSC) and/or other drugs to acutely dissociated auditory cortical neurons. Application of NMDA produced large inward currents whose profile was unchanged during the application of ACSF (e.g., in Fig. 2A). On the contrary, the application of either ACh or oxo on top of the NMDA application resulted in a reversible decrease of the $I_{NMDA}$ ($R = 42.3 \pm 2\%$, $n = 11$, and $R = 22.9 \pm 1.4\%$, $n = 8$, respectively; Figs. 2B and 2C) whose onset and offset kinetics were only slightly slower than the drug dispensing speed of the system ($\tau = 1089 \pm 28$ ms, $n = 11$, e.g. in the time expansion of Fig. 2B). Mean ± s.e.m. of $R$, the reduction induced by ACh or oxo is shown in Figure 2D.

### The cholinergic inhibition of $I_{NMDA}$ is not G-protein mediated

The resistance of cholinergic inhibition of $I_{NMDA}$ to atropine suggested that muscarinic receptors were not responsible for the effect. In order to determine whether the activation of other GTP-dependent protein (G-protein) receptors was responsible for the $I_{NMDA}$ inhibition we measured the effect of ACh on currents evoked by pressure application of NMDA using an intracellular solution containing the nonhydrolyzable analog of guanosine-di-phosphate, $GDP_\beta S$ (500 μM) to lock the α-subunit of trimeric G-protein complexes in a permanently inactive state. In the presence of $GDP_\beta S$ in the pipette solution the application of a low concentration ACh (10 nM) or oxo (10 nM) still induced a reversible decrease in the cEPSC $I_{NMDA}$ (e.g., in Figs. 3A and 3B). To test the possible effect of endogenous ACh, we determined the action of the ACh-esterase inhibitor physostigmine on the cEPSC. In the presence of $GDP_\beta S$ in the recording pipette, physostigmine reversibly decreased cEPSC amplitude, (10.6 ± 4% in 10 μM, $n = 4$, and 28.4 ± 5% in 50 μM, $n = 4$, $P < 0.05$, $t$-test, e.g., in Fig. 3C), raising the possibility that endogenous ACh reduces $I_{NMDA}$ in a G-protein-independent fashion, similar to exogenously applied ACh. Mean ± s.e.m. for the effects of ACh, oxo, or physostigmine on the cEPSC $I_{NMDA}$ amplitudes are shown in Figure 3D.

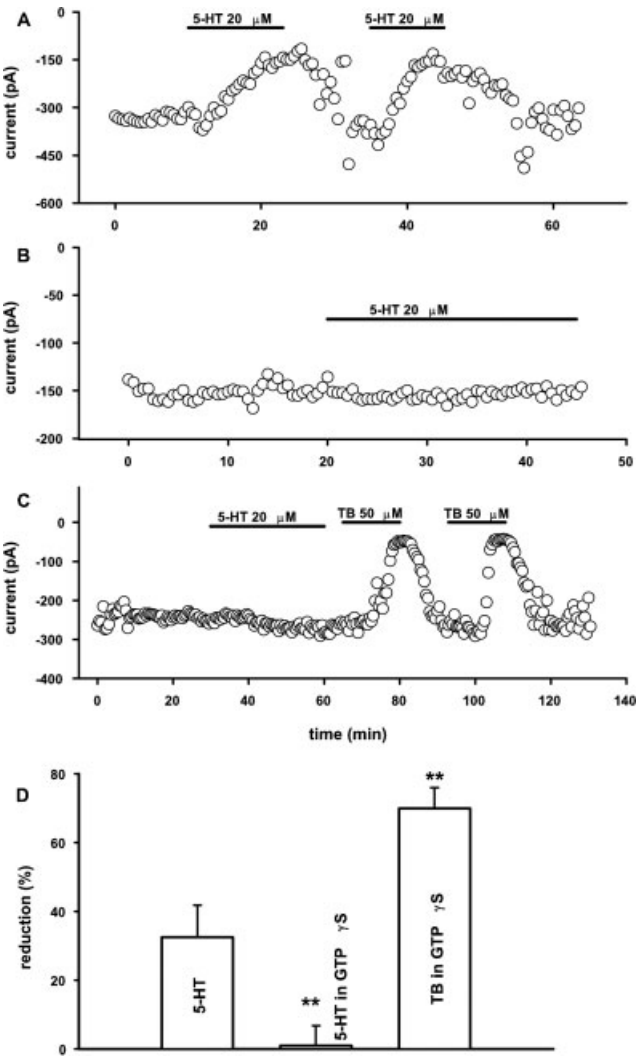


Fig. 5. G-proteins are activated with $GTP_\gamma S$ and tubocurarine still reduces $I_{NMDA}$. **A**: 5-HT (20 μM) decreases chemically evoked $I_{NMDA}$ in control, but not in the presence of $GTP_\gamma S$ (400 μM, **B**). **C**: Tubocurarine (50 μM) but not 5-HT inhibit chemically induced $I_{NMDA}$ in the presence of $GTP_\gamma S$. **D**: mean ± s.e.m. of the reduction by 5-HT in control ($n = 5$), serotonin in $GTP_\gamma S$ ($n = 5$), and tubocurarine (50 μM) in $GTP_\gamma S$ ($n = 4$).

### Nicotinic agonists and antagonists inhibit $I_{NMDA}$

To determine whether muscarinic drugs selectively inhibited $I_{NMDA}$, we tested the effect of the nicotine and tubocurarine—prototype nicotinic agonist and antagonist, respectively—on the amplitude of the cEPSC. Application of nicotine or tubocurarine consistently inhibited $I_{NMDA}$ in brain slices as well as in dissociated cells (Fig. 4). In the presence of $GDP_\beta S$, nicotine (10 μM) reversibly inhibited NMDAR-mediated cEPSC in brain slices ($R = 58 \pm 3\%$, $n = 7$) as well as in dissociated cells ($R = 35.5 \pm 8\%$, $n = 5$), as shown as examples in Figures 4A and 4B. Similarly, tubocurarine, also in the presence of $GDP_\beta S$, reversibly decreased cEPSC amplitude in brain slices (e.g.,

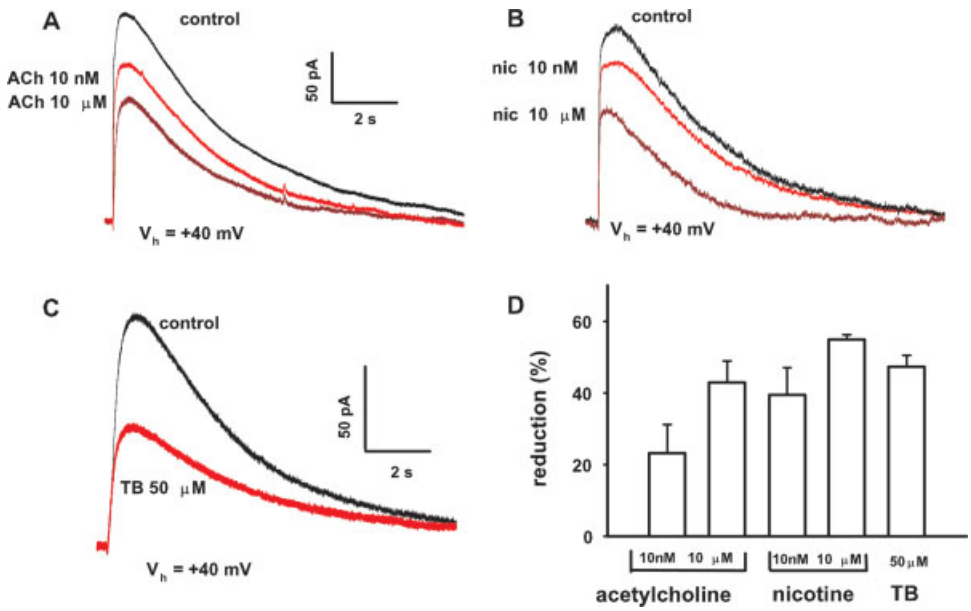


Fig. 6. The inhibition of $I_{NMDA}$ is not voltage-dependent. **A–C**: Representative traces showing that ACh (10 nM or 10 μM), nicotine (10 nM or 10 μM), or tubocurarine (50 μM), respectively inhibit cEPSC $I_{NMDA}$ in brain slices at a holding voltage $V_h$ = + 40 mV. **D**: Mean ± s.e.m. of the reduction induced by ACh (10 nM or 10 μM), nicotine (10 or 50 μM), or tubocurarine (50 μM).

in Fig. 4C) as well as in dissociated cells (e.g., in Fig. 4D). Tubocurarine also inhibited electrically evoked $I_{NMDA}$ in brain slices (38.2 ± 6.6%, $n$ = 6, e.g., in Fig. 4E).

For ascertaining whether the inhibiting effect of physostigmine was due to its block of cholinesterase as suggested by the experiment in Figures 3C and 3D, or was rather a direct block of $I_{NMDA}$ we also measured the effect of physostigmine bath-applications on cEPSC $I_{NMDA}$ in dissociated cells. Unexpectedly, physostigmine significantly decreased $I_{NMDA}$ (e.g., in Fig. 4F), indicative of a direct postsynaptic effect. Mean ± s.e.m. for the tubocurarine, nicotine and physostigmine inhibition of chemically induced $I_{NMDA}$ are summarized in the bar graphs in Figures 4G and 4H for brain slices and dissociated cells, respectively.

To verify the effectiveness of intracellular dialysis, we used an intracellular solution with $GTP_{\gamma}S$ (400 μM)—which like or $GDP_{\beta}S$ locks the α-subunit of trimeric G-protein complex, this time in a permanently active state—to test the effect of serotonin on the chemically evoked $I_{NMDA}$ in recordings from cells of the medial prefrontal cortex, where 5-HT postsynaptically decreases NMDAR-mediated current through activation of the G-protein mediated 5-HT1A receptor (Yuen et al., 2005). As expected, we found that application of 5-HT (20 μM) reduced $I_{NMDA}$ in control pipette solution (e.g., in Fig. 5A) but not in the presence of $GTP_{\gamma}S$ (e.g., in Figs. 5B and 5C). On the contrary, tubocurarine (50 μM) still depressed $I_{NMDA}$ even in the presence of $GTP_{\gamma}S$ in the pipette solution (e.g., in Fig. 5C). The presence of GTPγS in the recording pipette produced similar results also in the auditory cortex, blocking any effect of 5-HT ($R$ = 3 ± 2%, n.s., $n$ = 4, data not shown), without changing the extent of the $I_{NMDA}$ inhibition induced by tubocurarine (50 μM, $R$ = 50 ± 4%, $n$ = 8, $P < 0.05$, paired Student's $t$-test).

## Mechanism of the cholinergic inhibition of $I_{NMDA}$

NMDARs receptors are subject to voltage-dependent block by neurotransmitters and modulators which carry multiple positive electric charges, and may block the channel pore in an activity- and voltage-dependent fashion (Cui et al., 2006). Furthermore, the NMDAR is subject to a block by $Mg^{2+}$ ions which is relieved at depolarized potential (Mayer et al., 1984). We tested the possibility that the cholinergic inhibition was voltage-dependent by recording cEPSC $I_{NMDA}$ at a depolarized holding potential ($V_h$) = + 40 mV. At this holding potential, cEPSC were recorded as outward currents, consistent with a reversal voltage for $I_{NMDA}$ around 0 mV. Application of ACh, nicotine or tubocurarine inhibited $I_{NMDA}$ to a similar extent measured at $V_h$ = −40 mV ($n$ = 4), suggesting that the reduction was not voltage-dependent (representative e.g., in Figs. 6A–6C, respectively). In particular, ACh produced a dose-dependent response whose maximal effect was similar to that produced by either nicotine (10 nM–10 μM, $n$ = 6 each) or tubocurarine (50 μM, $n$ = 4). Summary of these results are reported as mean ± s.e.m. in the graph bar in Figure 6D.

Since all cholinergic drugs that we tested effectively inhibited $I_{NMDA}$ we decided to test the effect of atropine (10 μM) on the amplitude of cEPSC in the presence of $GTP_{\gamma}S$ (400 μM). Atropine applications did

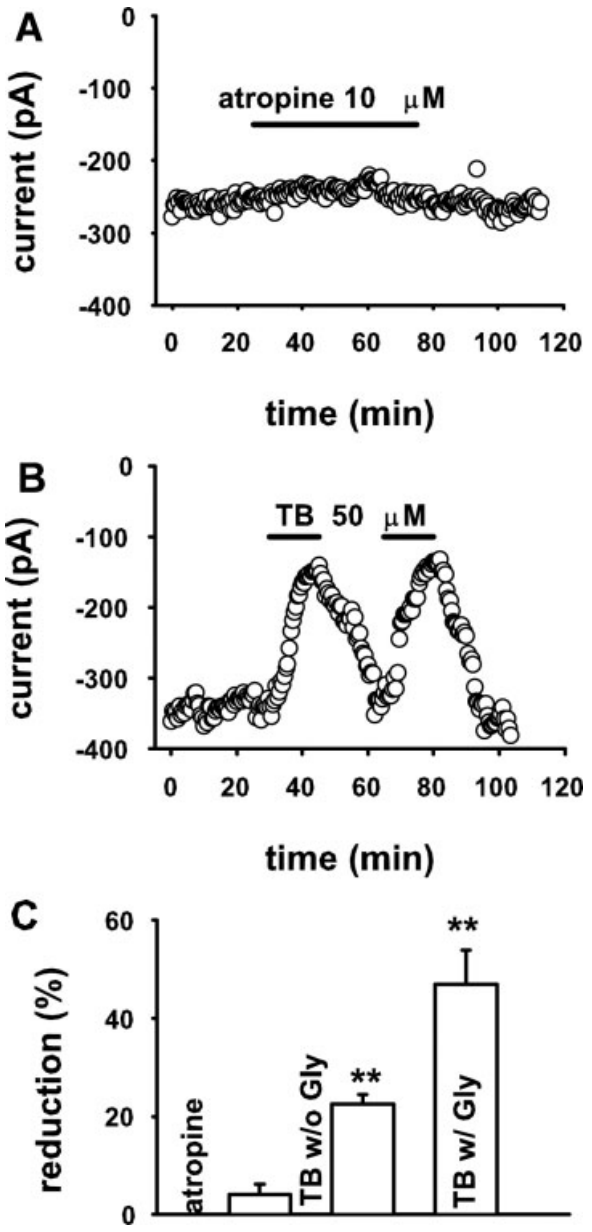


Fig. 7. Effect of cholinergic antagonists. Recordings in the presence of $GTP_{\gamma}S$ (400 μM) in the pipette solution. **A**: atropine (10 μM) was unable to reduce $I_{NMDA}$, whereas tubocurarine (50 μM, **B**) produced a completely reversible reduction in $I_{NMDA}$ in two consecutive applications. **C**: Bar graphs report mean ± s.e.m. of the $I_{NMDA}$ reduction by atropine, tubocurarine without glycine, or tubocurarine with glycine ($n$ = 4).

not change cEPSC amplitude (e.g., in Fig. 7A), whereas in the same recording conditions (GTPγS in the pipette solution) tubocurarine reliably induced a reversible reduction of $I_{NMDA}$, shown as example in Figure 7B.

The NR1 subunit of the NMDAR has a binding site for the aminoacid glycine and serine, whose presence is required for opening the channel following glutamate binding (Parsons et al., 1998). We considered the possibility that cholinergic inhibition of $I_{NMDA}$ operated by modifying glycine or serine binding. To test this hypothesis, we measured cEPSC $I_{NMDA}$ in ACSF or after application of glycine (20 μM) to the extracellular solution, with a pipette solution containing $GDP_{\beta}S$ (500 μM). In the presence of glycine, the tubocurarine-induced decrease in cEPSC $I_{NMDA}$ amplitude more than doubled (mean ± s.e.m. in the bar graph in Fig. 7C). An example of time course of the effects of tubocurarine on the cEPSC $I_{NMDA}$ amplitude in the presence or in the absence of glycine is shown as example in Fig. 8A. For investigating in more depth tubocurarine-induced inhibition, we obtained a dose response of the inhibition by tubocurarine in the presence or in the absence of 20 μM glycine. We found that while in the nominal absence of glycine tubocurarine induced only a relatively modest decrease of the $I_{NMDA}$, in the presence of 20 μM glycine tubocurarine induced a reduction that was consistently larger throughout the dose-response curve, leading, for saturating doses of tubocurarine, to approximately the same current regardless of the presence or absence of glycine, around 40% of the maximal current in glycine (Fig. 8B). A plot of the nonnormalized $I_{NMDA}$ percentage reduction by tubocurarine (Fig. 8C) showed the greater potency of the tubocurarine reduction in the presence of glycine (maximum reduction by tubocurarine was 31 ± 2.5% in control vs. 56 ± 7% in 20 μM glycine). The complexity of the interaction between tubocurarine and glycine is illustrated by the change of the normalized dose-response curve, showing a glycine-induced right-shift (Fig. 7D, $IC50_{tubocurarine}$(control) = 8 ± 1 nM vs. $IC50_{tubocurarine}$(gly) = 98 ± 7 nM), with no change in the Hill coefficient (Fig. 8D). Small differences between $I_{NMDA}$ reductions obtained with the same concentration of tubocurarine measured in $GTP_{\gamma}S$ vs. $GDP_{\beta}S$ were not statistically significant. These results are compatible with the hypothesis of a non-competitive mechanism of inhibition whereby tubocurarine displaces glycine from its binding site.

## DISCUSSION

Nicotinic agonists are suggested to inhibit $I_{NMDA}$ through a noncompetitive mechanism (O'Dell and Christensen, 1988). Our data confirm that nicotinic agonist inhibit NMDAR-mediated currents, and show for the first time that also the nicotinic antagonists tubocurarine, oxo, the endogenous neurotransmitter ACh, as well as the cholinesterase inhibitor physostigmine, all decrease $I_{NMDA}$ in an atropine-insensitive manner, suggestive of a non-muscarinic mechanism. The unchanged PPR of the synaptic responses suggested a postsynaptic site of the effect, confirmed by the cholinergic reduction of currents evoked by the

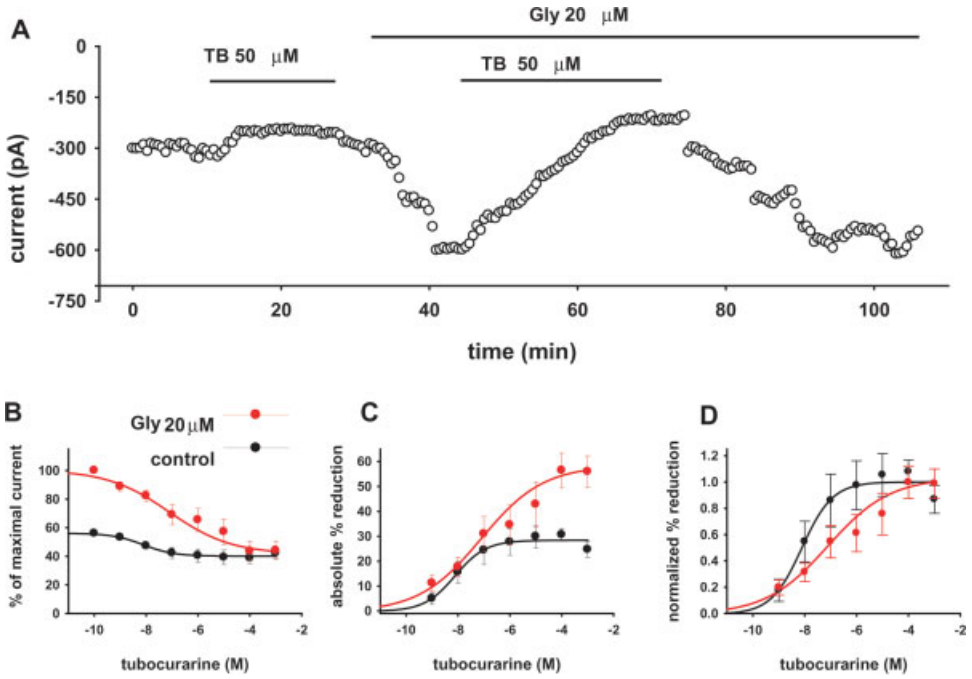


Fig. 8. Tubocurarine inhibits $I_{NMDA}$ in a glycine-dependent manner. Recordings in the presence of $GDP_{\beta}S$ (500 μM) in the pipette solution **A**: Example of time course illustrating that tubocurarine (50 μM) exerts a modest reduction of $I_{NMDA}$ in control. As expected, application of glycine (20 μM) greatly increases $I_{NMDA}$. Subsequent application of the same concentration of tubocurarine in the presence of glycine produces a much larger percent of inhibition, bringing $I_{NMDA}$ to the minimum recorded current. All effects were completely reversible. **B–D**: Dose response of tubocurarine in the presence (red lines and symbols) or in the absence (black lines and symbols) of glycine (20 μM). B: Normalizing currents to the maximum current in the presence of glycine shows that saturating doses of tubocurarine bring $I_{NMDA}$ to a minimal level independent on the presence of glycine (~ 40% of the maximal current in glycine). C: Tubocurarine potency, measured as the maximum percentage reduction of the control current, is greatly increased in the presence of 20 μM glycine. D: the presence of glycine brings about large differences in the dose response of $I_{NMDA}$ to tubocurarine.

application of NMDA in brain slices as well as in dissociated neurons. The rapid kinetic of the reduction of $I_{NMDA}$ induced by ACh and oxo in dissociated neurons suggested a direct interaction between the cholinergic drugs and the NMDAR.

## Mechanism

Since several drugs and ions operate a voltage-dependent block of NMDAR-dependent currents, we tested whether cholinergics would inhibit $I_{NMDA}$ at depolarized potentials to similar extent of the blockage in a hyperpolarized cell. No substantial differences were detected in the extent of the blockage at $V_h$ = +40 mV vs. $V_h$ = −40 mV, failing to demonstrate any voltage dependence of the inhibition.

Similar to the inhibition induced by ACh and oxo, the reduction in $I_{NMDA}$ following nicotine and tubocurarine applications were not blocked by the presence of drugs preventing a large range of intracellular second-messenger cascades, suggesting that nicotinic and muscarinic substances alike might inhibit NMDAR-mediated currents using similar mechanisms.

We considered the possibility that cholinergic drugs interact at the glycine site by displacing the NMDAR coagonist glycine. Because of its high effectiveness and reversibility as $I_{NMDA}$ blocker, tubocurarine was selected as prototype inhibitor. Although tubocurarine induced a large $I_{NMDA}$ reduction in the presence of the NMDAR coagonist glycine, the same substance induced only a modest but measurable, dose-dependent inhibition in nominal absence of glycine suggesting that tubocurarine might compete with this amino-acid displacing glycine from its binding site at the NR1 subunit. The specific mechanism of inhibition might differ for other cholinergic drugs.

Our data did not allow to assess whether $I_{NMDA}$ is physiologically inhibited by ACh, as initially suggested by the inhibition of synaptic $I_{NMDA}$ by the cholinesterase blocker physostigmine, since physostigmine itself inhibited $I_{NMDA}$ also in dissociated cells, indicative of its direct interaction with the NMDAR. Our data do not completely rule out the possibility of a protein–protein interaction between the NMDAR and functional or nonfunctional ionotropic channels like those formed by the nicotinic α9 and/or α10 subunits, which possess a mixed muscarinic–nicotinic pharmacology (Baker et al., 2004; Lustig, 2006).

The cholinergic reduction of NMDARs is less surprising if we consider that NMDAR the "inverse"

interaction (the block of nicotinic channels by NMDA antagonists) has already been reported in several studies (Aracava et al., 2005; Buisson and Bertrand, 1998a,b; Plazas et al., 2007) suggesting that at least nicotinic and NMDA ligands somehow overlap at least partly in their ligand affinities, although the specific mechanisms of their interactions might differ.

These data would suggest an alternative interpretation to the finding that in the sensory neocortex, nicotine, but also carbachol, inhibit $I_{NMDA}$ (Levy et al., 2006). Differences with our work might be due to the different cortical area (somatosensory vs. auditory) or different cortical layer (L V vs. L II/III), or shorter duration of the drug application. Our data also supply a simple explanation to a series of observations reporting that exposure to nicotine protects form NMDAR-mediated glutamate toxicity in a number of preparations (Ferchmin et al., 2003; Prendergast et al., 2001; Rezvani and Levin, 2003).

### Physiological significance

Microdialysis studies have shown that the concentration of ACh measured in the presence of cholinesterase blockers is in the order of a fraction of micromolar (McIntyre et al., 2003). Even in the case that actual brain concentration of ACh would be two orders of magnitude lower, the significant reduction of $I_{NMDA}$ observed for a concentration of ACh as low as 10 nM indicates that ACh could significantly inhibit tonically at least extrasynaptic NMDARs at physiological concentrations, whereas the transient reduction of synaptic NMDAR-mediated conductance would be possible following intense ACh release by cholinergic varicosities located in the neighborhood of glutamatergic synapses.

A cholinergic reduction of NMDARs could be an alternative or complementary mechanism for the induction of neocortical long-term depression which is associated to cholinergic modulation (Kirkwood et al., 1999). Considering that NMDARs and nicotinic receptors have high $Ca^{2+}$ permeabilites, it is tempting to speculate that the effect of the increase in the physiologic concentrations of ACh in the neocortex would shift the distribution of neuronal $Ca^{2+}$ entry from NMDAR-rich to nicotine receptors-rich neuronal regions, potentially introducing a parallel shift in the loci of synaptic plasticity.

## REFERENCES


Aizenman E, Tang LH, Reynolds IJ. 1991 Effects of nicotinic agonists on the NMDA receptor. Brain Res 551(1/2):355–357.

Alkondon M, Albuquerque EX. 2004. The nicotinic acetylcholine receptor subtypes and their function in the hippocampus and cerebral cortex. Prog Brain Res 145:109–120.

Aracava Y, Pereira EF, Maelicke A, Albuquerque EX. 2005. Memantine blocks alpha7* nicotinic acetylcholine receptors more potently than *N*-methyl-D-aspartate receptors in rat hippocampal neurons. J Pharmacol Exp Ther 312:1195–1205.

Aramakis VB, Bandrowski AE, Ashe JH. 1997. Activation of muscarinic receptors modulates NMDA receptor-mediated responses in auditory cortex. Exp Brain Res 113:484–496.

Aramakis VB, Bandrowski AE, Ashe JH. 1999. Role of muscarinic receptors. G-proteins, and intracellular messengers in muscarinic modulation of NMDA receptor-mediated synaptic transmission. Synapse 32:262–275.

Aramakis VB, Metherate R. 1998. Nicotine selectively enhances NMDA receptor-mediated synaptic transmission during postnatal development in sensory neocortex. J Neurosci 18:8485–8495.

Atzori M, Kanold PO, Pineda JC, Flores-Hernandez J, Paz RD. 2005. Dopamine prevents muscarinic-induced decrease of glutamate release in the auditory cortex. Neuroscience 134:1153–1165.

Atzori M, Lei S, Evans DI, Kanold PO, Phillips-Tansey E, McIntyre O, McBain CJ. 2001. Differential synaptic processing separates stationary from transient inputs to the auditory cortex. Nat Neurosci 4:1230–1237.

Baker ER, Zwart R, Sher E, Millar NS. 2004. Pharmacological properties of alpha 9 alpha 10 nicotinic acetylcholine receptors revealed by heterologous expression of subunit chimeras. Mol Pharmacol 65:453–460.

Beech DJ. 1993. Inhibitory effects of histamine and bradykinin on calcium current in smooth muscle cells isolated from guinea-pig ileum. J Physiol 463:565–583.

Buisson B, Bertrand D. 1998a. Allosteric modulation of neuronal nicotinic acetylcholine receptors. J Physiol (Paris) 92:89–100.

Buisson B, Bertrand D. 1998b. Open-channel blockers at the human alpha4beta2 neuronal nicotinic acetylcholine receptor. Mol Pharmacol 53:555–563.

Burgos-Robles A, Vidal-Gonzalez I, Santini E, Quirk GJ. 2007. Consolidation of fear extinction requires NMDA receptor-dependent bursting in the ventromedial prefrontal cortex. Neuron 53:871–880.

Castellano C, Cestari V, Ciamei A. 2001. NMDA receptors and learning and memory processes. Curr Drug Targets 2:273–283.

Chub N, Moore LE, O'Donovan MJ. 1998. Comparison of NMDA-induced membrane potential oscillations and spontaneous rhythmic activity in the chick spinal cord. Ann N Y Acad Sci 860: 467–469.

Cox CL, Metherate R, Weinberger NM, Ashe JH. 1992. Synaptic potentials and effects of amino acid antagonists in the auditory cortex. Brain Res Bull 28:401–410.

Cui C, Xu M, Atzori M. 2006. Voltage-dependent Block of NMDA receptors by dopamine D1 receptor ligands. Mol Pharmacol 70:1761–1770.

Ferchmin PA, Perez D, Eterovic VA, de Vellis J. 2003. Nicotinic receptors differentially regulate *N*-methyl-D-aspartate damage in acute hippocampal slices. J Pharmacol Exp Ther 305:1071–1078.

Flores-Hernandez J, Cepeda C, Hernandez-Echeagaray E, Calvert CR, Jokel ES, Fienberg AA, Greengard P, Levine MS. 2002. Dopamine enhancement of NMDA currents in dissociated medium-sized striatal neurons: Role of D1 receptors and DARPP-32. J Neurophysiol 88:3010–3020.

Jones SV, Barker JL, Bonner TI, Buckley NJ, Brann MR. 1988. Electrophysiological characterization of cloned m1 muscarinic receptors expressed in A9 L cells. Proc Natl Acad Sci USA 85: 4056–4060.

Kirkwood A, Rozas C, Kirkwood J, Perez F, Bear MF. 1999. Modulation of long-term synaptic depression in visual cortex by acetylcholine and norepinephrine. J Neurosci 19:1599–1609.

Levy RB, Reyes AD, Aoki C. 2006. Nicotinic and muscarinic reduction of unitary excitatory postsynaptic potentials in sensory cortex; dual intracellular recording in vitro. J Neurophysiol 95: 2155–2166.

Lustig LR. 2006. Nicotinic acetylcholine receptor structure and function in the efferent auditory system. Anat Rec A Discov Mol Cell Evol Biol 288:424–434.

Mash DC, Potter LT. 1986. Autoradiographic localization of M1 and M2 muscarine receptors in the rat brain. Neuroscience 19:551–564.

Mayer ML, Westbrook GL, Guthrie PB. 1984. Voltage-dependent block by Mg2+ of NMDA responses in spinal cord neurones. Nature 309:261–263.

McIntyre CK, Marriott LK, Gold PE. 2003. Patterns of brain acetylcholine release predict individual differences in preferred learning strategies in rats. Neurobiol Learn Mem 79:177–183.

Metherate R, Ashe JH. 1991. Basal forebrain stimulation modifies auditory cortex responsiveness by an action at muscarinic receptors. Brain Res 559:163–167.

Metherate R, Ashe JH. 1993a. Ionic flux contributions to neocortical slow waves and nucleus basalis-mediated activation: Whole-cell recordings in vivo. J Neurosci 13:5312–5323.
Metherate R, Ashe JH. 1993b. Nucleus basalis stimulation facilitates thalamocortical synaptic transmission in the rat auditory cortex. Synapse 14:132–143.
Metherate R, Ashe JH. 1994. Facilitation of an NMDA receptor-mediated EPSP by paired-pulse stimulation in rat neocortex via depression of GABAergic IPSPs. J Physiol 481(Part 2):331–348.
Metherate R, Ashe JH, Weinberger NM. 1990. Acetylcholine modifies neuronal acoustic rate-level functions in guinea pig auditory cortex by an action at muscarinic receptors. Synapse 6:364–368.
Metherate R, Weinberger NM. 1989. Acetylcholine produces stimulus-specific receptive field alterations in cat auditory cortex. Brain Res 480(1/2):372–377.
Metherate R, Weinberger NM. 1990. Cholinergic modulation of responses to single tones produces tone- specific receptive field alterations in cat auditory cortex. Synapse 6:133–145.
Nicoll RA, Malenka RC. 1999. Expression mechanisms underlying NMDA receptor-dependent long-term potentiation. Ann N Y Acad Sci 868:515–525.
O'Dell TJ, Christensen BN. 1988. Mecamylamine is a selective noncompetitive antagonist of *N*-methyl-D-aspartate- and aspartate-induced currents in horizontal cells dissociated from the catfish retina. Neurosci Lett 94(1–2):93–98.
Parsons CG, Danysz W, Hesselink M, Hartmann S, Lorenz B, Wollenburg C, Quack G. 1998. Modulation of NMDA receptors by glycine–introduction to some basic aspects and recent developments. Amino Acids 14(1/3):207–216.
Plazas PV, Savino J, Kracun S, Gomez-Casati ME, Katz E, Parsons CG, Millar NS, Elgoyhen AB. 2007. Inhibition of the alpha9alpha10 nicotinic cholinergic receptor by neramexane, an open channel blocker of N-methyl-D-aspartate receptors. Eur J Pharmacol 566(1/3):11–19.
Prendergast MA, Harris BR, Mayer S, Holley RC, Hauser KF, Littleton JM. 2001. Chronic nicotine exposure reduces *N*-methyl-D-aspartate receptor-mediated damage in the hippocampus without altering calcium accumulation or extrusion: Evidence of calbindin-D28K overexpression. Neuroscience 102:75–85.
Rezvani AH, Levin ED. 2003. Nicotinic-glutamatergic interactions and attentional performance on an operant visual signal detection task in female rats. Eur J Pharmacol 465(1/2):83–90.
Rutkowski RG, Miasnikov AA. 2003.Weinberger NM, Characterisation of multiple physiological fields within the anatomical core of rat auditory cortex. Hear Res 181(1/2):116–130.
Voytko ML. 1996. Cognitive functions of the basal forebrain cholinergic system in monkeys: Memory or attention? Behav Brain Res 75(1/2):13–25.
Voytko ML, Olton DS, Richardson RT, Gorman LK, Tobin JR, Price DL. 1994. Basal forebrain lesions in monkeys disrupt attention but not learning and memory. J Neurosci 14:167–186.
Vulfius CA, Ryazansky VD, Krasts IV, Ilyasov FE. 1998. Intracellular Ca2+ modulates Cl-current evoked by acetylcholine in Lymnaea neurons. Neurosci Lett 249:5–8.
Yuen EY, Jiang Q, Chen P, Gu Z, Feng J, Yan Z. 2005. Serotonin 5-HT1A receptors regulate NMDA receptor channels through a microtubule-dependent mechanism. J Neurosci 25: 5488–5501.